An automated hydrogel screening platform

Caleb Johnston[1] Aaron Clasky[1] Nasrudeen Oladimeji[1] Mohammad Nazeri[1] Sheldon Mei[1] Frank Gu[1]
[1][University of Toronto, 27 King's College Circle, Toronto, Ontario, Canada, M5S 1A1]

Correspondence to: Frank Gu f.gu@utoronto.ca

1. Introduction

Hydrogels are soft materials comprised of a crosslinked polymer network and continuous water phase and are used in various biomedical applications [1-3]. Due to their chemical, physical, and temporal complexity, discovering and optimizing hydrogel materials is difficult and laborious [4, 5]. Automation has been demonstrated to accelerate development in related fields of drug discovery [6] and lipid nanoparticles [7], but to date the automatic preparation, capture and analysis of soft materials such as hydrogels has not been shown.

Here, we present an automated hydrogel screening system built around a liquid handling robot augmented with custom hardware and an integrated imaging system. Our platform enables rapid screening of hydrogel formulations with corresponding time-resolved images in standard multiwell plates. Our imaging algorithm automatically identifies gels to accelerate down-selection of promising formulations.

2. Substantial

To enable high-throughput hydrogel screening, we designed an automated workflow centered on liquid-handling automation. A commercially available open-source liquid-handling robot (Opentrons) was used as the core platform, as it provides sufficient positional accuracy and volume control for microliter scale dispensing while remaining modifiable with custom hardware and software.

The experimental setup (Fig. 1) integrates the liquid handler and an endoscopic camera through a custom mount, enabling in situ imaging immediately after dispensing. Hydrogel precursor solutions are dispensed into standard 96-well plates.

Automation is achieved through scripted liquid-handling protocols that control dispensing order, volumes, and timing, along with synchronized image acquisition. Validation experiments demonstrate reproducible bead formation across multiple wells and runs (Appendix A). The system has a throughput of approximately 200 unique data points per hour, generating full gelation time series data (0-20min) for 28 distinct formulations. To date, the platform has been used to screen thousands of hydrogel formulations spanning a broad parameter space of precursor compositions, concentrations, and dispensing conditions (Fig. 2).

The hardware automation is linked to an image analysis program that identifies gels present in the wells. The program fits a curve to the well and feeds the processed images to a ResNet18 model [8], fine-tuned on a dataset of 13,000+ examples of gelled and non-gelled images generated in-house. The model achieves close agreement with human visual assessment (sensitivity: 98.3%, specificity: 97.2%, precision: 96.2%; accuracy: 97.7%) (Fig. 3).

3.1 Related work

Nazeri et al. [9] developed the foundational hardware platform; an Opentrons OT-2 liquid handler with a custom 3D-printed pick-and-place apparatus and integrated USB camera, upon which the abstract improves and modifies by adding an updated camera mount and a software-based image classifier to enable true high-throughput screening of hydrogels

Soh et al. [10] demonstrated liquid-handling automation for viscometry, showing how automated platforms can use proxy methods to quantify material properties. While bulk viscosity can be used to track sol-gel transitions under some conditions, the current abstract assesses gel formation in real time, providing both spatial and temporal data to track dynamic changes in the gelation process.

Cheong et al. [11] showed ML-guided hydrogel formulation optimization on a miniaturized system with a focus on drug release kinetics, whereas the abstract addresses the upstream challenge of rapid gelation screening across broad compositional spaces to identify gel-forming conditions before functional characterization.

3.2 *Figures*

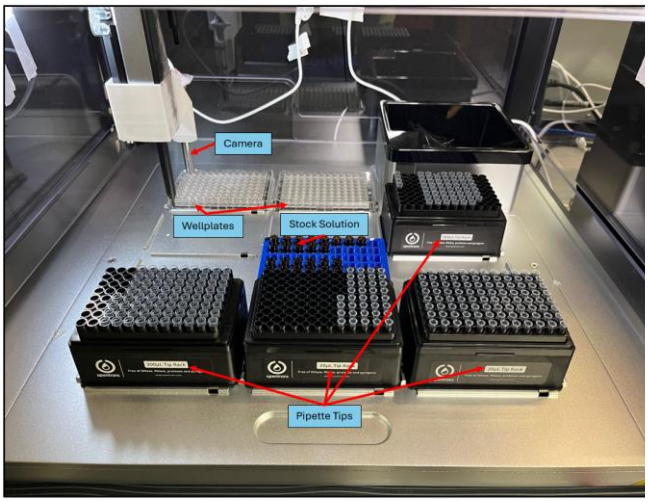

Fig. 1: Opentrons layout for hydrogel screening platform.

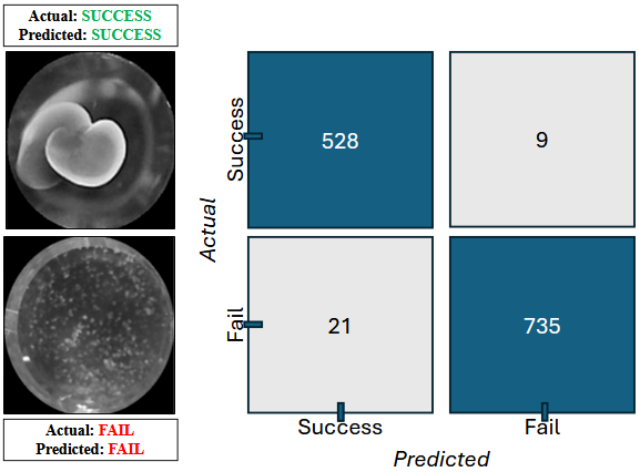

Fig. 3: Image processing algorithm automatically intakes and sorts microwell images (left) into successful gels (SUCCESS) or failed formulations (FAIL). The 2x2 confusion matrix (right) demonstrates the algorithm achieves 97.7% accuracy in its classification.

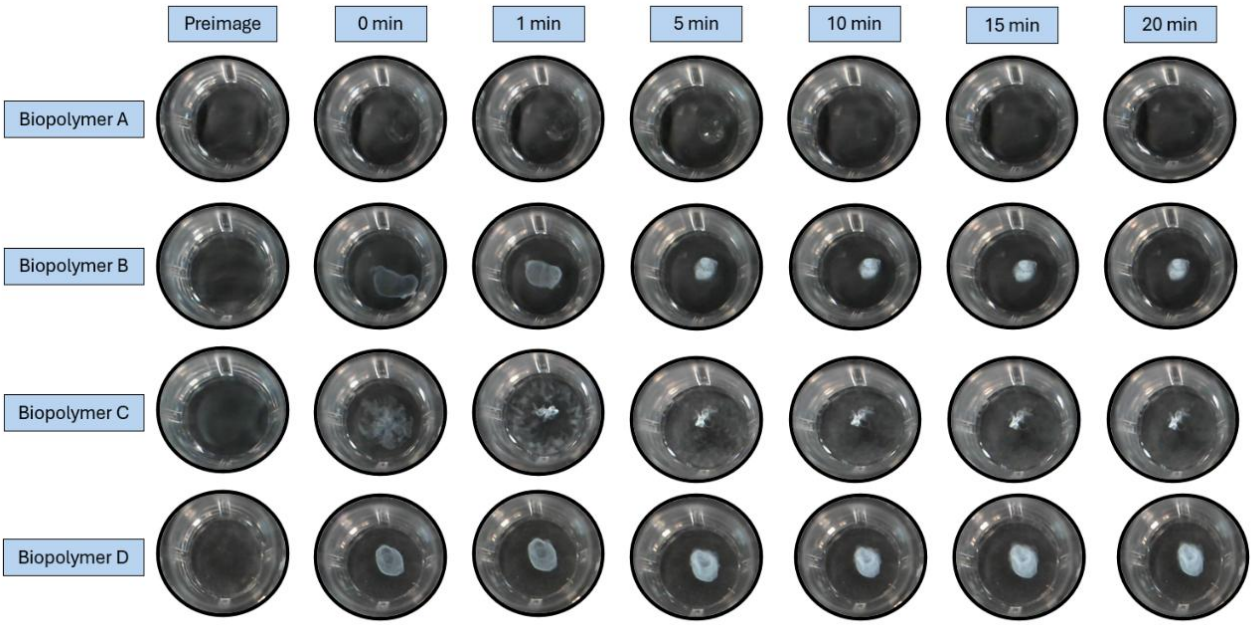

Fig. 2: Example gelation time series for four representative biopolymers, including “non-gelling” (A) and gelling (B-D) combinations

Acknowledgments

The authors acknowledge the use of the Formulations Self-Driving Laboratory (SDL-5) at the Acceleration Consortium for providing essential facilities and technical support. This research is part of the University of Toronto's Acceleration Consortium, which receives funding from the Canada First Research Excellence Fund (CFREF). NSERC Discovery Grant (Spon Ref: RGPIN-2019-06441, Fund# 506723) - Canada First Res Excellence Fund - AC: Scientific Strategy (n).

References

[1] S. Dong *et al.*, "Therapeutic Hydrogels: Properties and Biomedical Applications," *Chem. Rev.*, vol. 125, no. 18, pp. 8835–8920, Sep. 2025, doi: 10.1021/acs.chemrev.5c00182.

[2] X. Lin, X. Zhang, Y. Wang, W. Chen, Z. Zhu, and S. Wang, "Hydrogels and hydrogel-based drug delivery systems for promoting refractory wound healing: Applications and prospects," *International Journal of Biological Macromolecules*, vol. 285, p. 138098, Jan. 2025, doi: 10.1016/j.ijbiomac.2024.138098.

[3] A. S. Hoffman, "Hydrogels for biomedical applications," *Advanced Drug Delivery Reviews*, vol. 54, no. 1, pp. 3–12, Jan. 2002, doi: 10.1016/S0169-409X(01)00239-3.

[4] A. Negro, T. Cherbuin, and M. P. Lutolf, "3D Inkjet Printing of Complex, Cell-Laden Hydrogel Structures," *Sci Rep*, vol. 8, no. 1, p. 17099, Nov. 2018, doi: 10.1038/s41598-018-35504-2.

[5] H. Fan and J. P. Gong, "Fabrication of Bioinspired Hydrogels: Challenges and Opportunities," *Macromolecules*, vol. 53, no. 8, pp. 2769–2782, Apr. 2020, doi: 10.1021/acs.macromol.0c00238.

[6] S. Sudhahar *et al.*, "An experimentally validated approach to automated biological evidence generation in drug discovery using knowledge graphs," *Nat Commun*, vol. 15, no. 1, p. 5703, Jul. 2024, doi: 10.1038/s41467-024-50024-6.

[7] S. Sudhahar *et al.*, "An experimentally validated approach to automated biological evidence generation in drug discovery using knowledge graphs," *Nat Commun*, vol. 15, no. 1, p. 5703, Jul. 2024, doi: 10.1038/s41467-024-50024-6.

[8] K. He, X. Zhang, S. Ren, and J. Sun, "Deep Residual Learning for Image Recognition," in 2016 IEEE Conference on Computer Vision and Pattern Recognition (CVPR), Las Vegas, NV, USA: IEEE, Jun. 2016, pp. 770–778. doi: 10.1109/CVPR.2016.90.

[9] M. Nazeri, J. Watchorn, S. Mei, A. Zhang, C. Allen, and F. Gu, "Leveraging flexible pipette-based tool changes to transform liquid handling systems into dual-function sample preparation and imaging platforms" June 2025, *HardwareX*, vol 22, e00653. doi: 10.1016/j.ohx.2025.e00653.

[10] B. W. Soh *et al.*, "Opentrons for automated and high-throughput viscometry," *Digital Discovery*, vol. 4, no. 3, pp. 711–722, 2025, doi: 10.1039/D4DD00368C.

[11] E. Cheong, D. C. Radford, and A. J. Gormley, "Automated active learning to optimize hydrogel drug release profiles," *Journal of Controlled Release*, vol. 391, p. 114602, Mar. 2026, doi: 10.1016/j.jconrel.2026.114602.

Appendix A. Validation

The following appendix demonstrates the effects of different parameters on the generation of gel beads on the gel crosslinking platform. All studies were conducted with Biopolymer D and gelator in MilliQ water.

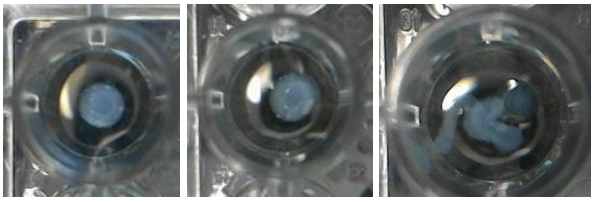

8 µL 9 µL **10µL**

Fig. A1: Effect of droplet volume (µl).

3 **2.5** 2

Fig. A2: Effect of gantry height (mm).

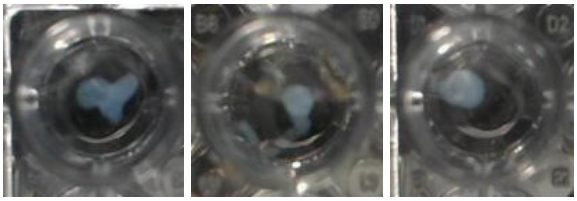

0.4 **0.5** 0.6

Fig. A3: Effect of flowrate (ml/min).

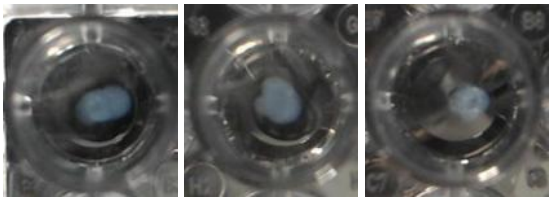

70 50 **30**

Fig. A4: Effect of moverate (mm/min).

0.5% 0.25%

Fig. A5. Effect of polymer concentration (%w/v)